Scientia Iranica F (2023) 30(6), 2235–2244

Sharif University of Technology
Scientia Iranica
Transactions F: Nanotechnology
http://scientiairanica.sharif.edu

Impact of viscous dissipation on MHD darcy-forchheimer nanoliquid flow comprising gyrotactic microorganisms past a nonlinear extending surface

M. Batool[a,*], S. Akhter[a,b], S. Ahmad[a,c], K. Ali[c], and M. Ashraf [a]

a. *Center for Advanced Studies in Pure and Applied Mathematics (CASPAM), Bahauddin Zakariya University, Multan 60800, Pakistan.*
b. *Department of Mathematics, COMSATS University (Islamabad), Sahiwal, Pakistan.*
c. *Department of Basic Sciences and Humanities, Muhammad Nawaz Sharif University of Engineering and Technology, Multan 60000, Pakistan.*

Received 7 September 2021; received in revised form 7 October 2022; accepted 21 November 2022

KEYWORDS
Darcy-Forchheimer;
Bioconvection;
Viscous dissipation;
Nonlinear stretching sheet;
Gyrotactic microorganisms.

Abstract. In the current study, the Magnetohydrodynamics (MHD) flow problem of Darcy-Forchheimer nano-liquid containing motile microorganisms with viscous dissipation impact past a nonlinear elongated sheet is addressed. Inclusion of gyrotactic microorganisms in nanoliquid helps boost up the thermal efficiency of numerous micro-biological systems. An iterative solution to the single-phase flow problem is attained using Successive Over Relaxation (SOR) procedure. The impacts of the leading parameters on the flow velocity, temperature, density, and concentration of motile microbes are considered and depicted in tables and graphs using MATLAB. Further, a comparison table is developed to check the accuracy of the numerical results of the flow problem under consideration. Increment in the value of the Forchheimer parameter causes the reduction of the velocity distribution. According to the findings, the Lewis number and Brownian motion parameters tend to enhance the rate of mass transport.

© 2023 Sharif University of Technology. All rights reserved.

1. Introduction

Nanoliquid is vastly used in different fields of medicine, chemical processes, heat transfer devices, chillers, cooling systems, and other industrial applications. Initially, Choi [1] found that a combined mixture of micro metallic particles and conventional base fluids would form a new kind of liquid known as nanoliquid. This new type of engineering liquid has a greater capacity of heat transfer than the conventional base fluids. In case the Reynolds number is greater than 1, the flow is considered nonlinear. Under such circumstances, it becomes impossible to ignore the impacts of inertia. The non-Darcian model of permeable media is obtained from classical Darcian model that includes inertial drag, vorticity diffusion impacts, inertial drag, and their combination, as well. In order to demonstrate the impression of boundary as well as inertia, Forchheimer [2] developed a square velocity term added to the expression of velocity. Muskat [3] called this term "Forchheimer term", which is valid for high Reynolds numbers. Darcy-Forchheimer theory was employed by Seddeek [4] to investigate the mixed convection Darcy-Forchheimer flow with thermophoresis and viscous dissipation impact through porous media. Sajid et al. [5]

*. *Corresponding author. Tel.: +92 3336001058*
E-mail address: maria.batool34@yahoo.com (M. Batool)

doi: 10.24200/sci.2022.59018.6018

found the solution to the problem of the flow of Darcy-Forchheimer Maxwell nanoliquid on a stretching linear shallow using the shooting technique. Sheikholeslami et al. [6–8] numerically interpreted the nanofluid performance in a solar Linear Fresnel Reflector (LFR) system, heat storage with honeycomb configuration using nanoparticles, and solar system equipped with innovative hybrid nanofluid.

Saif et al. [9] analyzed the Darcy-Forchheimer viscous nanofluid flow past an elongating curved surface through a penetrable region. Nasir et al. [10] investigated the flow problem of thin film 2D Darcy-Forchheimer nanofluid past a flat unsteady stretchable surface in a porous medium. Khan et al. [11] studied the problem of micropolar 3D MHD (Magnetohydrodynamics) Darcy-Forchheimer nanoliquid Carbon Nano-Tubes (CNTs) flowing through horizontal and parallel plates in a porous region. Ganesh et al. [12] scrutinized the MHD Darcy-Forchheimer flow of nanofluid past a sheet in a thermally stratified porous medium. They solved the flow problem through he Runge-Kutta method of order four along with shooting technique. Hayat et al. [13] numerically examined the nanoliquid flow with the thermophoresis impact and Brownian motion under Darcy-Forchheimer relationship. Sadiq and Hayat [14] addressed the problem of MHD Darcy-Forchheimer two-dimensional flow due to the stretched surface.

Muhammad et al. [15] investigated the boundary-layer MHD flow of the Maxwell nanoliquid generated by a stretching surface in a porous medium under the effect of uniform magnetic field. Hayat et al. [16] scrutinized the boundary layer flow problem of Darcy-Forchheimer Williamson nanomaterial on a bidirectional nonlinearly stretching surface in a porous region. To this end, they adopted Homotopy Analysis Method (HAM) to generate a numerical solution for the governing nonlinear system of flow problem. Zakaullah et al. [17] computed the numerical solution of Darcy-Forchheimer nanofluid flow problem with partial slip impacts using the shooting methodology. Moreover, they discovered that the temperature and concentration of nanoparticles exhibited expanding behaviors at larger values of Forchheimer parameter. Turk and Tezer-Sezgin [18] addressed the flow problem of micropolar nanoliquid inside a square under the impact of magnetic field and computed its numerical solution using Finite Element Method (FEM). Shafiq et al. [19] scrutinized the special impacts of thermal slip and Arrhenius activation energy on the flow of Darcy-Forchheimer nanoliquid resulting from a stretching surface. Of note, in recent years, some other investigations on the Darcy-Forchheimer flow have been published [20–22].

The swimming of gyrotactic microorganisms gives rise to the phenomenon of bioconvection. The spectacle of bioconvection boosts up the microscale mixing and stability of nanoparticles. Effective heat distribution results from the stabilized nanoparticles. Shahid et al. [23] numerically inspected the flow of blood comprising motile microbes passing through a stretching and penetrable region. They computed the numerical solution of blood flow problem based on Successive Taylor Series Linearization Method (STSLM). Waqas et al. [24] developed Buongiorno's model to investigate the flow characteristics of the MHD Williamson nanoliquid due to a porous wedge containing gyrotactic microorganisms. The numerical solution of this time-dependent flow problem was achieved by the shooting method. In the presence of motile microorganisms, Sohail and Naz [25] obtained the numerical solution of the flow problem regarding the Maxwell nanofluid with thermal radiation impact using HAM. Some recent relevant studies can be found in [26–29].

The present study of Darcy-Forchheimer nanofluid flow has different valuable applications in biomedical sciences and biotechnology. To the best of our knowledge, given that the numerical investigation of viscous dissipation in Darcy-Forchheimer nanofluid flow containing gyrotactic microbes based on Successive Over Relaxation (SOR) technique has not been studied before, we found the right motivation to conduct this study. This paper addresses the behavior of numerous parameters affecting the MHD flow of Darcy-Forchheimer nanoliquid containing gyrotactic microorganisms under the effect of viscous dissipation. The numerical solutions are presented using the figures and tables of various pertinent parameters associated with the problem through MATLAB.

2. Mathematical formulation

Let us assume the steady viscous 2D incompressible Darcy-Forchheimer flow of the MHD nanofluid resulting from a stretching sheet which behaves nonlinearly. The sheet has motion along the x-axis at the stretching velocity of $U_{bn} = b_0 x^m$, where m and $b_0 > 0$ are constant terms.

The geometry of the modeled flow problem is given in Figure 1.

The system of differential equations representing the current flow problem is represented in the formulaic form as:

$$\frac{\partial u}{\partial x} + \frac{\partial v}{\partial y} = 0, \tag{1}$$

$$u\frac{\partial u}{\partial x} + v\frac{\partial u}{\partial y} = \nu\left(\frac{\partial^2 u}{\partial y^2}\right) - \left(\frac{\sigma_{Ec} B_0^2 x^{m-1}}{\rho_{Fl}} + \frac{\nu}{K_*}\right) u - \frac{c_B}{\sqrt{K_*}} u^2, \tag{2}$$

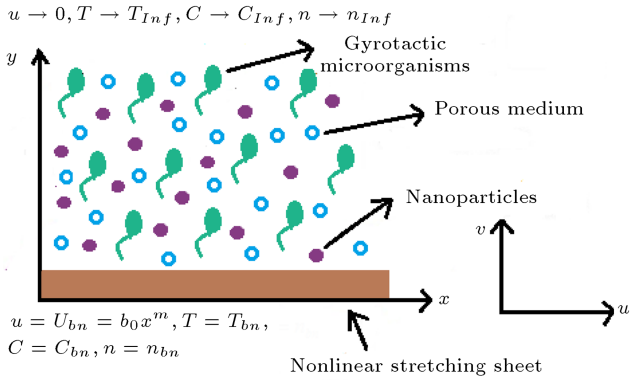

Figure 1. The geometry of the flow problem.

$$u\frac{\partial T}{\partial x}+v\frac{\partial T}{\partial y}=\alpha\frac{\partial^2 T}{\partial y^2}+\frac{(\rho c)_{Np}}{(\rho c)_{Fl}}\times\left\{D_{BM}\left(\frac{\partial C}{\partial y}\frac{\partial T}{\partial y}\right)+\frac{D_{Tp}}{T_{Inf}}\left(\frac{\partial T}{\partial y}\right)^2\right\}+\frac{\nu}{c_p}\left(\frac{\partial u}{\partial y}\right)^2, \tag{3}$$

$$u\frac{\partial C}{\partial x}+v\frac{\partial C}{\partial y}=D_{BM}\frac{\partial^2 C}{\partial y^2}+\frac{D_{Tp}}{T_{Inf}}\frac{\partial^2 T}{\partial y^2}, \tag{4}$$

$$u\frac{\partial n}{\partial x}+v\frac{\partial n}{\partial y}+\frac{b_{ch}W_{cs}}{(C_{bn}-C_{Inf})}\left\{\frac{\partial}{\partial y}\left(n\frac{\partial C}{\partial y}\right)\right\}=D_{GM}\frac{\partial^2 n}{\partial y^2}. \tag{5}$$

Boundary Conditions (BCs) related to the above equations are:

$$u=U_{bn}=b_0x^m,\quad v=0,$$
$$T=T_{bn},\quad C=C_{bn},\quad n=n_{bn}\quad \text{at}\quad y=0, \tag{6}$$
$$u\to 0,\quad T\to T_{Inf},\quad C\to C_{Inf},\quad n\to n_{Inf}$$
$$\text{as}\quad y\to\infty. \tag{7}$$

Let us define the dimensionless quantities as:

$$\eta=\frac{1}{2}\sqrt{\frac{2b_0(m+1)\rho_{Fl}}{\mu}}x^{\frac{m-1}{2}}y,$$
$$\theta(\eta)=\frac{T-T_{Inf}}{T_{bn}-T_{Inf}},\qquad \chi(\eta)=\frac{n-n_{Inf}}{n_{bn}-n_{Inf}},$$
$$\phi(\eta)=\frac{C-C_{Inf}}{C_{bn}-C_{Inf}},\qquad u=b_0x^m f'(\eta),$$
$$v=-\frac{1}{2}\sqrt{2b_0(m+1)\nu}x^{\frac{m-1}{2}}. \tag{8}$$

The velocity components $u=\frac{\partial\psi}{\partial y}$ and $v=-\frac{\partial\psi}{\partial x}$ provide assistance to develop the stream function ψ, and η denotes the dimensionless similarity variable. The components u and v can satisfy Eq. (1) in the form of ψ. The transformation specified in Eq. (8) can be exploited to convert Eqs. (2)–(5) into the Ordinary Differential Equations (ODEs) given below:

$$f'''+ff''-\left[\frac{2m}{m+1}\right]f'^2-Me^2f'-\lambda f'-Fr(f')^2=0, \tag{9}$$

$$\theta''+Pr\left[Nb\theta'\phi'+Nt\theta'^2+\theta' f\right]+PrEcf''^2=0, \tag{10}$$

$$\phi''+\frac{Nt}{Nb}\theta''+LePr(f'\phi')=0, \tag{11}$$

$$\chi''+Sc(f\chi')-Pe\left[\chi'\phi'+\phi''(\chi+\sigma)\right]=0. \tag{12}$$

Also, BCs written in Eqs. (6) and (7) have dimensionless forms that are given below:

$$f(0)=0,\quad f'(0)=1,\quad \theta(0)=1,$$
$$\phi(0)=1,\qquad \chi(0)=1,\quad \text{at}\quad \eta=0, \tag{13}$$
$$f'=0,\quad \theta=0,\quad \phi=0,\quad \chi=0,\quad \text{as}\quad \eta\to\infty, \tag{14}$$

where the primes symbolize the derivative with respect to η. Further, Me is the magnetic parameter, Le the Lewis number, Nt the thermophoresis parameter, λ the porosity parameter, Ec the Eckert number, Pr the Prandtl number, Sc the Schmidt number, Nb the parameter of Brownian motion, Pe the Peclet number, σ_{Ec} a constant term, and Fr the Forchheimer parameter, all taking the following mathematical forms:

$$Nt=\frac{(\rho c)_{Np}D_{Th}(T_{bn}-T_{Inf})}{(\rho c)_{Fl}\upsilon T_{Inf}},$$
$$Nb=\frac{(\rho c)_{Np}D_{BM}(C_{bn}-C_{Inf})}{(\rho c)_{Fl}\upsilon},$$
$$Pr=\frac{\upsilon}{\alpha},\quad Ec=\frac{(u_{bn})^2}{c_p(T_{bn}-T_{Inf})},\quad Sc=\frac{\upsilon}{D_{GM}},$$
$$Le=\frac{\upsilon}{D_{BM}},\quad Me=\sqrt{\frac{2\sigma_{Ec}B_0^2}{b_0\rho_{Fl}(m+1)}},$$
$$Pe=\frac{b_{ch}W_{cs}}{D_{GM}},\qquad \sigma_{Ec}=\frac{n_{Inf}}{(n_{bn}-n_{Inf})},$$
$$\lambda=\frac{2\upsilon}{K_*b_0(m+1)x^{m-1}},\quad Fr=\frac{2c_Bx}{K_*^{\frac{1}{2}}(m+1)}. \tag{15}$$

3. Numerical computation

Many researchers are constantly contributing in various fields to find numerical solutions to the nonlinear modeled problems. In our problem, numerical elucidation of the resulting nonlinear ODEs Eqs. (9)–(12) involving BCs described in Eqs. (13) and (14) is accomplished through an SOR-based methodology. This procedure was adopted in this study owing to its ability to facilitate fast convergence, given the complexity of computing the analytical solution of nonlinear differential equations of higher order. A detailed discussion on our numerical technique can be seen in our previous papers [30–35].

To find the numerical solution to the coupled system of nonlinear ODEs, Finite Difference Method (FDM) was employed. Since the ODE given in Eq. (9) is of third-order type, its order is reduced by putting $f' = r$. Finally, the resulting system of equations with their BCs takes the following form:

$$r'' + fr' - \left[\frac{2m}{m+1}\right] r^2 - Me^2 r - \lambda r - Fr(r)^2 = 0, \quad (16)$$

$$\theta'' + Pr\left[Nb\theta'\phi' + Nt\theta'^2 + \theta' f\right] + PrEcr'^2 = 0, \quad (17)$$

$$\phi'' + \frac{Nt}{Nb}\theta'' + LePr(f\phi') = 0, \quad (18)$$

$$\chi'' + Sc(f\chi') - Pe\left[\chi'\phi' + \phi''(\chi + \sigma_{Ec})\right] = 0. \quad (19)$$

The BCs get the form of:

$$f(0) = 0, \quad r(0) = 1, \quad \theta(0) = 1, \quad \phi(0) = 1,$$

$$\chi(0) = 1, \quad \text{at} \quad \eta = 0,$$

$$r = 0, \quad \theta = 0, \quad \phi = 0, \quad \chi = 0, \quad \text{as} \quad \eta \to \infty. \quad (20)$$

Firstly, the domain $[0, \infty)$ of the flow problem under study is discretized for the numerical manipulation of the above-mentioned system of equations. In order to integrate the equation $f' = r$, Simpson's numerical iterative process is employed. In addition, a well-known central difference approximation is employed to discretize the involved derivatives in Eqs. (16)–(20), and an iterative solution is found through the SOR. This iterative scheme is terminated when:

$$\max(\|r_{j+1} - r_j\|_2, \|f_{j+1} - f_j\|_2, \|\theta_{j+1} - \theta_j\|_2,$$

$$\|\phi_{j+1} - \phi_j\|_2, \|\chi_{j+1} - \chi_j\|_2) < Tol_{itr},$$

is satisfied through up to four consecutive iterations.

4. Results and discussion

This section presents our outcomes through physical elucidations. The relevant flow model dimensionless Eqs. (9)–(12) are numerically treated based on the SOR method. The velocity $f'(\eta)$, motile microorganisms (microbes) density distribution $\chi(\eta)$, concentration $\phi(\eta)$, and temperature $\theta(\eta)$ display asymptotic appearance against the well-adjusted step size η. The movements of microorganisms and nanoparticles are independent of each other. The motion of nanoparticles is due to the Brownian and thermophoresis effects while the bioconvection phenomenon within the flow causes the motion of the mobile microorganisms. Unlike the nanoparticles, the microorganisms exhibit self-propelled movements. The impacts of the physical parameters on the shear stress, mass transport rate, density number of motile microbes, and heat transport rate are also examined and tabularized.

Figures 2–5 illustrate the motile microbes' density, velocity, concentration, and temperature profiles, respectively, at different values of magnetic field parameter Me. As evidently seen in these figures, the magnetic parameter enhances the microorganisms' density, temperature, and concentration, while it de-

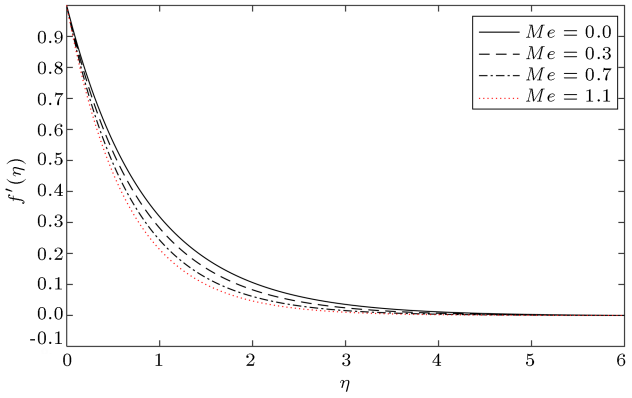

Figure 2. Velocity distribution for different values of Me by setting $\lambda = 0.2$, $Fr = 0.2$, $Pr = 1.2$, $Nb = 0.1$, $Nt = 0.2$, $m = 1.3$, $Ec = 0.1$, $\sigma_{Ec} = 0.2$, $Le = 2$, $Pe = 0.1$, and $Sc = 2.2$.

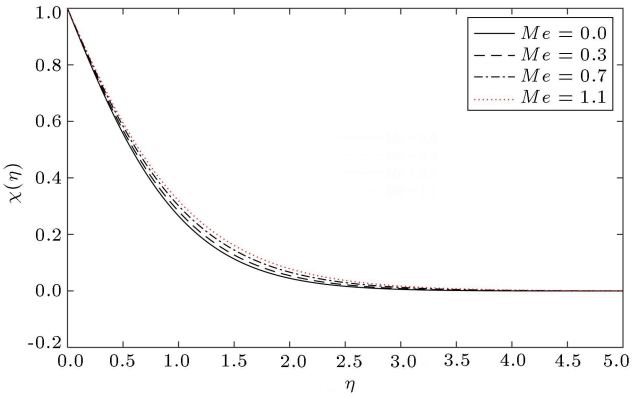

Figure 3. Microorganism's density distribution for different values of Me by setting $\lambda = 0.2$, $Fr = 0.2$, $Pr = 1.2$, $Nb = 0.1$, $Nt = 0.2$, $m = 1.3$, $Ec = 0.1$, $\sigma_{Ec} = 0.2$, $Le = 2$, $Pe = 0.1$, and $Sc = 2.2$.

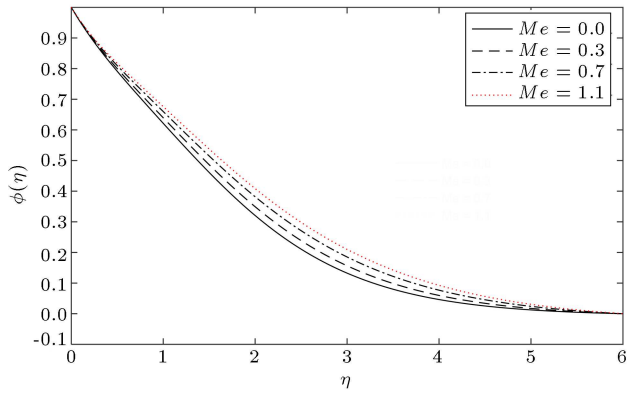

Figure 4. Microorganism's concentration for different values of Me by setting $\lambda = 0.2$, $Fr = 0.2$, $Pr = 1.2$, $Nb = 0.1$, $Nt = 0.2$, $m = 1.3$, $Ec = 0.1$, $\sigma_{Ec} = 0.2$, $Le = 2$, $Pe = 0.1$, and $Sc = 2.2$.

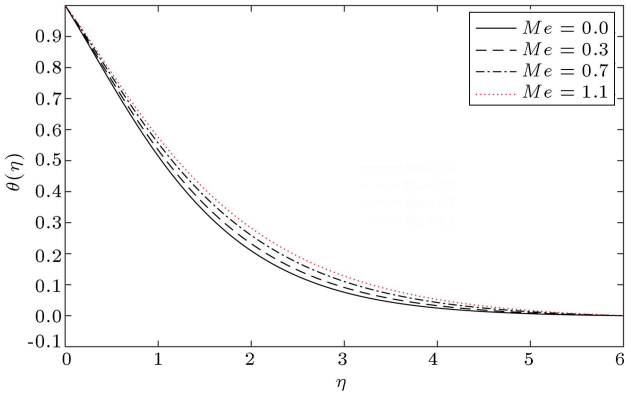

Figure 5. Temperature distribution for different values of Me by setting $\lambda = 0.2$, $Fr = 0.2$, $Pr = 1.2$, $Nb = 0.1$, $Nt = 0.2$, $m = 1.3$, $Ec = 0.1$, $\sigma_{Ec} = 0.2$, $Le = 2$, $Pe = 0.1$, and $Sc = 2.2$.

creases velocity. A retarding force is induced in the motion direction because of the applied magnetic field. This force strictly opposes the motion which causes a reduction in the fluid velocity. The same profiles are examined for porosity parameter, as appeared in Figures 6–9. Analysis of these figures reveals the same effects of porosity and magnetic parameters on the aforementioned profiles.

The impacts of local inertia or Forchheimer parameter on the profiles such as $f'(\eta)$, $\chi(\eta)$, $\theta(\eta)$, and $\phi(\eta)$ are portrayed in Figures 10–13. The velocity profile decreases under the effect of Forchheimer parameter, while the rest of them, i.e., the density, concentration, and temperature of the microbes, increase with an increase in this parameter. Both porosity and Forchheimer parameters act parallel to each other in terms of their effects on the dimensionless profiles. The porosity of the medium and surface drag are proportional to the Forchheimer parameter or inertial coefficient. For this reason, the resistive force increases, which in turn enhances the surface friction. Consequently, the raising values of Fr cause a decrease

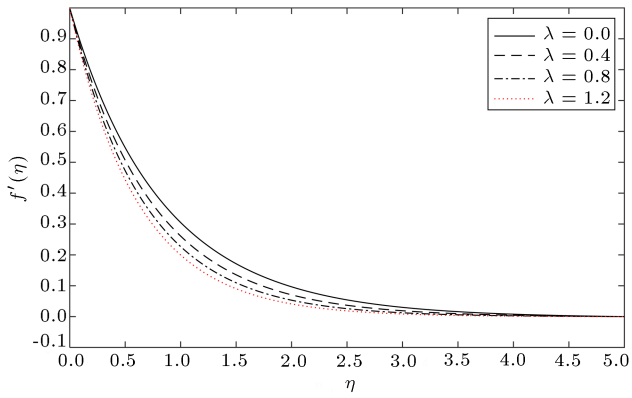

Figure 6. Velocity distribution for various values of λ by setting $Me = 0.3$, $Fr = 0.2$, $Pr = 2.2$, $Nb = 0.1$, $Nt = 0.2$, $m = 1.3$, $Ec = 0.1$, $\sigma_{Ec} = 0.2$, $Le = 1.9$, $Pe = 0.1$, and $Sc = 2$.

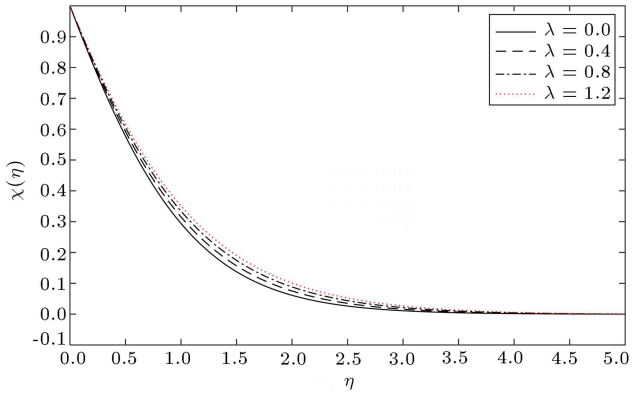

Figure 7. Microorganisms' density distribution for various values of λ by setting $Me = 0.3$, $Fr = 0.2$, $Pr = 2.2$, $Nb = 0.1$, $Nt = 0.2$, $m = 1.3$, $Ec = 0.1$, $\sigma_{Ec} = 0.2$, $Le = 1.9$, $Pe = 0.1$, and $Sc = 2$.

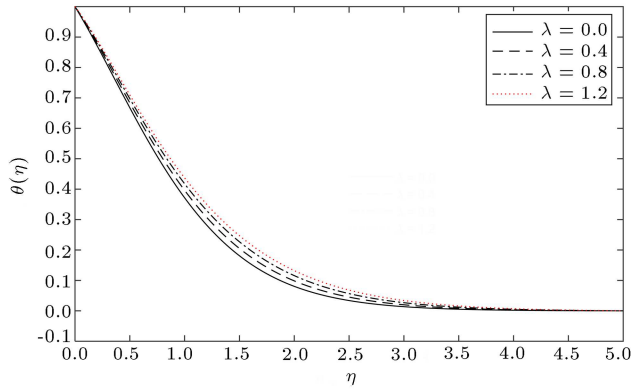

Figure 8. Temperature distribution for various values of λ by setting $Me = 0.3$, $Fr = 0.2$, $Pr = 2.2$, $Nb = 0.1$, $Nt = 0.2$, $m = 1.3$, $Ec = 0.1$, $\sigma_{Ec} = 0.2$, $Le = 1.9$, $Pe = 0.1$, and $Sc = 2$.

in the velocity and an increase in the density of the motile microbe.

To validate the obtained code, a numerical data comparison is presented in Table 1. The outcomes are correlated with those presented by Rasool et al. [36].

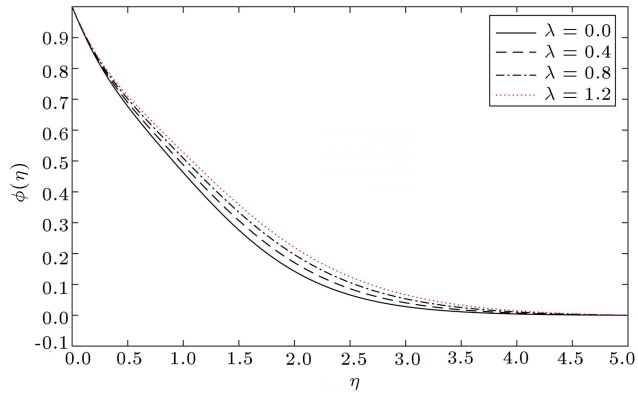

Figure 9. Microorganism's concentration for various values of λ by setting $Me = 0.3$, $Fr = 0.2$, $Pr = 2.2$, $Nb = 0.1$, $Nt = 0.2$, $m = 1.3$, $Ec = 0.1$, $\sigma_{Ec} = 0.2$, $Le = 1.9$, $Pe = 0.1$, and $Sc = 2$.

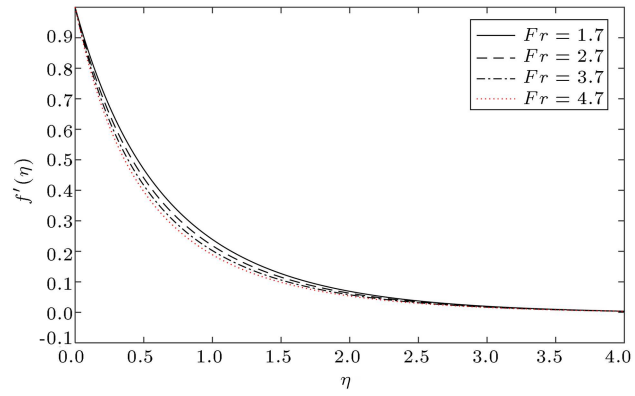

Figure 10. Velocity distribution for various values of Fr by setting $Me = 0.3$, $\lambda = 0.2$, $Pr = 1.2$, $Nb = 0.1$, $Nt = 0.2$, $m = 1.3$, $Ec = 0.1$, $\sigma_{Ec} = 0.2$, $Le = 2$, $Pe = 0.1$, and $Sc = 2.2$.

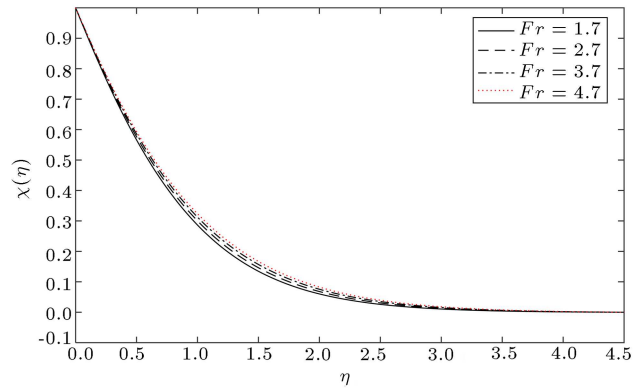

Figure 11. Microorganism's density distribution for various values of Fr by setting $Me = 0.3$, $\lambda = 0.2$, $Pr = 1.2$, $Nb = 0.1$, $Nt = 0.2$, $m = 1.3$, $Ec = 0.1$, $\sigma_{Ec} = 0.2$, $Le = 2$, $Pe = 0.1$, and $Sc = 2.2$.

The results match the limiting cases for distinct values of Forchheimer parameter. The satisfying correlation of the results in Table 1 ensures the accuracy of our numerical solutions.

Tables 2–5 are provided to check out the impacts

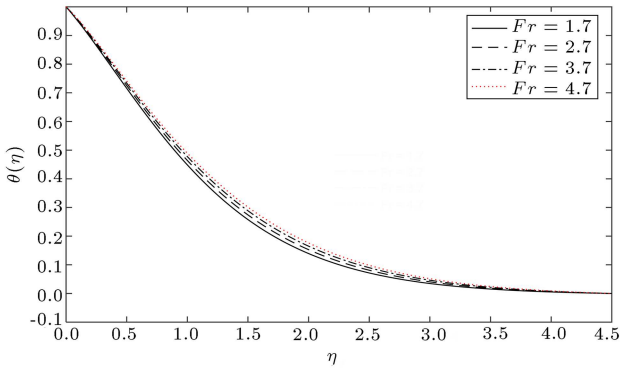

Figure 12. Temperature distribution for various values of Fr by setting $Me = 0.3$, $\lambda = 0.2$, $Pr = 1.2$, $Nb = 0.1$, $Nt = 0.2$, $m = 1.3$, $Ec = 0.1$, $\sigma_{Ec} = 0.2$, $Le = 2$, $Pe = 0.1$, and $Sc = 2.2$.

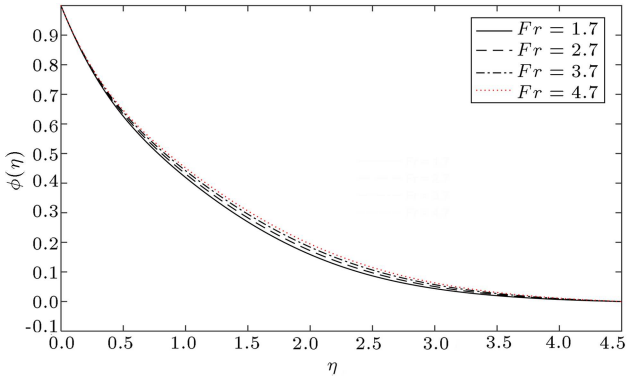

Figure 13. Microorganism's concentration for various values of Fr by setting $Me = 0.3$, $\lambda = 0.2$, $Pr = 1.2$, $Nb = 0.1$, $Nt = 0.2$, $m = 1.3$, $Ec = 0.1$, $\sigma_{Ec} = 0.2$, $Le = 2$, $Pe = 0.1$, and $Sc = 2.2$.

of the preeminent parameters on the local motile density number $\chi'(0)$, local Sherwood number $\phi'(0)$, skin friction coefficient $f''(0)$, and local Nusselt number $\theta'(0)$. The variation of the skin friction for several parameters is depicted in Table 2. Here, the various values of the porosity, magnetic, and Forchheimer parameters enhance the skin friction. Table 3 examines the impacts of some parameters like Nt, Nb, λ, Fr, Ec, and Me on the Nusselt number. The values of $\theta'(0)$ are reduced under the effect of these parameters, while magnetic, porosity, and thermophoresis parameters tend to devaluate the mass transport rate on the sheet surface. On the contrary, as shown in Table 4, the Lewis number, Brownian motion, and Forchheimer parameter cause a substantial increase in the Sherwood number (mass transfer rate).

The desired results can be obtained by providing the suitable values to the preeminent parameters. The sizes of the pores can affect the local density of the microorganisms. To be specific, in case the sizes of pores are so small such that the tiny organisms do not cross them easily, the bioconvection may not occur. In order to avoid this situation, it is suggested to

Table 1. Comparison with Rasool et al. [36] by setting $Ec = 0$, $\sigma_{Ec} = 0$, $Pe = 0$, and $Sc = 0$.

Fr	$-Re_x^{-1/2} Nu_x$		$-Re_x^{-1/2} Sh_x$	
	Present	**Rasool et al. [36]**	**Present**	**Rasool et al. [36]**
0.0	0.5133	0.5115	0.4088	0.4085
0.6	0.4936	0.4953	0.3767	0.3925
1.2	0.4853	0.4814	0.3728	0.3789

Table 2. Variation in $f''(0)$ for different values of λ, Fr and Me.

λ	Me	Fr	$f''(0)$
0.0			−1.423938
0.3	0.2	0.9	−1.53581
0.5			−1.606089
	0.0		−1.423938
0.2	0.2	0.9	−1.499455
	0.4		−1.571352
		0.0	−1.267705
0.2	0.2	0.3	−1.349067
		0.6	−1.426118

Table 3. Variation in $-\theta'(0)$ against different values of Nt, Nb, λ, Fr, Ec, and Me.

Nt	Nb	λ	Fr	Ec	Me	$-\theta'(0)$
0.1						0.445417
0.2	0.2	0.2	0.9	0.1	0.2	0.415899
0.4						0.385252
	0.1					0.467118
0.1	0.2	0.2	0.9	0.1	0.2	0.432433
	0.4					0.391482
		0.0				0.456385
0.1	0.2	0.3	0.9	0.1	0.2	0.426793
		0.5				0.414351
			0.0			0.466133
0.1	0.2	0.2	0.3	0.1	0.2	0.446389
			0.6			0.437961
				0.0		0.499539
0.1	0.2	0.2	0.9	0.1	0.2	0.431806
				0.2		0.376081
					0.0	0.456385
0.1	0.2	0.2	0.9	0.1	0.2	0.432169
					0.4	0.419783

Table 4. Variation in $-\phi'(0)$ for different values of Me, λ, Nb, Nt, Le, and Fr.

Me	λ	Le	Nb	Nt	Fr	$-\phi'(0)$
0.0						0.430925
0.2	0.2	0.8	0.2	0.1	0.9	0.401441
0.4						0.397490
	0.0					0.430925
0.2	0.3	0.8	0.2	0.1	0.9	0.400779
	0.5					0.396747
		0.3				0.307160
0.2	0.2	0.5	0.2	0.1	0.9	0.311506
		0.7				0.363977
			0.1			0.328577
0.2	0.2	0.8	0.2	0.1	0.9	0.392125
			0.4			0.447677
				0.1		0.429622
0.1	0.2	0.8	0.2	0.2	0.9	0.335406
				0.4		0.237252
					0.0	0.431477
0.2	0.2	0.8	0.7	0.1	0.3	0.402987
					0.6	0.399828

use a medium with high porosity or much smaller permeability. Table 5 shows the impacts of Me, λ, Pe, Sc, and Fr on the density number $\chi'(0)$ of the motile microorganisms. It should be noted that the density of microbes is enhanced at higher values of Pe, Sc, and Fr. Contrarily, the magnetic and porosity parameters decrease the density of the microbes. As observed in the tabular analysis, the surface drags as well as $\chi'(0)$ increased on the sheet surface under the effect of the Forchheimer parameter.

5. Conclusions

The present research numerically investigated the Magnetohydrodynamics (MHD) Darcy-Forchheimer nanofluid flow due to nonlinear elongating sheet in

Table 5. Variation in $-\chi'(0)$ for different values of Me, λ, Pe, Sc, and Fr.

Me	λ	Pe	Sc	Fr	$-\chi'(0)$
0.0					0.455078
0.2	0.2	0.2	0.3	0.9	0.416871
0.4					0.410072
	0.0				0.455078
0.2	0.3	0.2	0.3	0.9	0.415472
	0.5				0.408550
		0.1			0.422488
0.2	0.2	0.3	0.3	0.9	0.442529
		0.5			0.498732
			0.1		0.398371
0.2	0.2	0.2	0.3	0.9	0.411313
			0.5		0.470771
				0.0	0.457298
0.2	0.2	0.2	0.3	0.3	0.420555
				0.6	0.415024

a porous medium. The magnetic effects not only maintained the temperature but also regulated the flow. The numerical outcomes were obtained through the Successive Over Relaxation (SOR) method. The major findings of this study are specified below:

- The magnetic parameter enhanced the density, temperature, and concentration of microorganisms, while it decreased the flow velocity;
- An increase in the Forchheimer parameter caused a decrease in the velocity and an increase in the density of the motile microbe;
- The porosity and thermophoresis parameters devaluated the mass transport rate on the sheet surface. On the contrary, the Lewis number and Brownian motion parameter caused a substantial increase in the Sherwood number (mass transfer rate);
- The Forchheimer parameter escalated $\chi'(0)$ on the sheet surface.

Abbreviations

u	x-component of velocity
v	y-component of velocity
μ	Dynamic viscosity
ν	Kinematic viscosity
ρ_{Fl}	Fluid's density
ρ_{Np}	Nanoparticles' density
T	Temperature
c_p	Specific heat
b_0	Positive constant
K_*	Permeability of medium
c_B	Drag force coefficient
D_{TP}	Thermo phoresis diffusion coefficient
D_{BM}	Brownian coefficient
D_{GM}	Microorganism diffusion coefficient
σ_{Ec}	Electric conductivity
T_{Inf}	Ambient temperature
W_{cs}	Maximum swimming speed of cell
T_{bn}	Temperature at surface of sheet
b_{ch}	Chemotaxis constant
α	Thermal diffusivity
Ec	Eckert number
B_0	Strength of magnetic field
n	Microorganisms' concentration
C	Volume fraction of nanoparticles
Me	Magnetic parameter
Pr	Prandtl number
Le	Lewis number
Sc	Schmidt number
Nb	Parameter of Brownian motion
Nt	Parameter of thermophoresis
Pe	Peclet number
λ	Porosity parameter
η	Dimensionless variable
Fr	Forchheimer parameter

References

1. Choi, S.U.S. "Enhancing thermal conductivity of fluids with nanoparticles developments and application of non-Newtonian flows", *ASME J. Heat Transfer*, **66**, pp. 99–105 (1997).
2. Forchheimer, P., "Wasserbewegungduch bodenzeitschrift ver ding", **45**, pp. 1782–1788 (1901).
3. Muskat, M., *The Flow of Homogenous Fluids Through Porous Media*, MI: Edwards (1995).
4. Seddeek, M.A. "Influence of viscous dissipation and thermophoresis on Darcy-Forchheimer mixed convection fluid in a saturated porous media", *J. Colloid. Interface Sci.*, **293**, pp. 137–142 (2006).
5. Sajid, T., Sagheer, M., Hussain, S., et al. "Darcy-Forchheimer flow of Maxwell nanofluid with nonlinear thermal radiation and activation energy", *AIP Adv.*, **8**, (2018). https://doi.org/10.1063/1.5019218

6. Sheikholeslami, M. and Ebrahimpour, Z. "Nanofluid performance in a solar LFR system involving turbulator applying numerical simulation", *Adv. Powder Technol.*, **33**(8) (2022). https://doi.org/10.1016/j.apt.2022.103669

7. Sheikholeslami, M."Analyzing melting process of paraffin through the heat storage with honeycomb configuration utilizing nanoparticles", *J. Energy Storage*, **52**, (2022). https://doi.org/10.1016/j.est.2022.104954

8. Sheikholeslami, M. "Numerical investigation of solar system equipped with innovative turbulator and hybrid nanofluid", *Sol. Energy Mater. Sol. Cells*, **243**, (2022). https://doi.org/10.1016/j.solmat.2022.111786

9. Saif, R.S., Hayat, T., Ellahi, R., et al. "Darcy-Forchheimer flow of nanofluid due to a curved stretching surface", *International Journal of Numerical Methods*, **29**, pp. 2–20 (2019).

10. Nasir, S., Shah, Z., Islam, S., et al. "Darcy-Forchheimer nanofluid thin film flow of SWCNTs and heat transfer analysis over an unsteady stretching sheet", *AIP Adv.* , **9** (2019). https://doi.org/10.1063/1.5083972

11. Khan, A., Shah, Z., Islam, S., et al. "Darcy-Forchheimer flow of MHD CNTs nanofluid radiative thermal behavior and convective non-uniform heat source/sink in the rotating frame with microstructure and inertial characteristics", *AIP Adv.*, **8**, (2018). https://doi.org/10.1063/1.5066223

12. Ganesh, N.V., Hakeem, A.K.A., and Ganga, B. "Darcy-Forchheimer flow of hydromagnetic nanofluid over a stretching/shrinking sheet in a thermally stratified porous medium with second order slip, viscous and Ohmic dissipation effects", *Ain Shams Eng. J.*, **9**, pp. 939–951 (2018).

13. Hayat, T., Haider, F., Muhammad, T., et al. "Numerical study for Darcy-Forchheimer flow of nanofluid due to an exponentially stretching curved surface", *Results Phys.*, **8**, pp. 764–771 (2018).

14. Sadiq, M.A. and Hayat, T. "Darcy-Forchheimer flow of magneto Maxwell liquid bounded by convectively heated sheet", *Results Phys.*, **6**, pp. 884–890 (2016).

15. Muhammad, T., Alsaedi, A., Shehzad, S.A., et al. "A revised model for Darcy-Forchheimer flow of Maxwell nanofluid subject to convective boundary condition", *Chinese J. Phys.*, **55**, pp. 963–976 (2017).

16. Hayat, T., Aziz, A., Muhammad, T., et al. "Darcy-Forchheimer three-dimensional flow of nanofluid over a convectively nonlinear stretching surface", *Commun. Theor. Phys.*, **68** (2017). https://doi.org/10.1088/0253-6102/68/3/387

17. Zakaullah, M., Capinnao, S.S., and Baleanu, D. "A numerical simulation for Darcy-Forchheimer flow of nanofluid by a rotating disk with partial slip effects", *Front. Phys.*, **7** (2020). https://doi.org/10.3389/fphy.2019.00219

18. Turk, O. and Tezer-Sezgin, M. "FEM solution to natural convection flow of a micropolar nanofluid in the presence of a magnetic field", *Meccanica*, **52**, pp. 889–901 (2017).

19. Shafiq, A., Rasool, G., and Khalique, C.M. "Significance of thermal slip and convective boundary conditions in three dimensional rotating Darcy-Forchheimer nanofluid flow", *Symmetry*, **12** (2020). http://dx.doi.org/10.3390/sym12050741

20. Saif, R.S., Hayat, T., Ellahi, R., et al. "Darcy-Forchheimer flow of nanofluid due to a curved stretching surface", *Int. J. Numer. Methods Heat Fluid Flow*, **29**, pp. 2–20 (2019).

21. Nasir, S., Shah, Z., Islam, S., et al. "Darcy-Forchheimer nanofluid thin film flow of SWCNTs and heat transfer analysis over an unsteady stretching sheet", *AIP Adv.*, **9**, (2019). https://doi.org/10.1063/1.5083972

22. Rasool, G., Zhang, T., Chamka, A.J., et al. "Entropy generation and consequences of binary chemical reaction on MHD Darcy-Forchheimer Williamson nanofluid flow over nonlinearly stretching surface", *Entropy*, **22**, (2020). https://doi.org/10.3390/e22010018

23. Shahid, A., Zhou, Z., Hassan, M., et al. "Computational study of magnetized blood flow in the presence of gyrotactic microorganisms propelled through a permeable capillary in a stretching motion", *Int. J. Multiscale Comput. Eng.* , **16**, pp. 409–426 (2018).

24. Waqas, H., Khan, S.U., Imran, M., et al. "Thermally developed Falkner-Skan bioconvection flow of a magnetized nanofluid in the presence of a motile gyrotactic microorganism: Buongiorno's nanofluid model", *Phys. Scr.*, **94**, (2019). https://doi.org/10.1088/1402-4896/ab2ddc

25. Sohail, M. and Naz, R. "On the onset of entropy generation for a nanofluid with thermal radiation and gyrotactic microorganisms through three-dimensional flows", *Phys. Scr.*, **95** (2020). https://doi.org/10.1088/1402-4896/ab3c3f

26. Sheikholeslami, M. and Ebrahimpour, Z. "Thermal improvement of linear Fresnel solar system utilizing Al_2O_3-water nanofluid and multi-way twisted tape", *Int. J. Therm. Sci.*, **176** (2022). https://doi.org/10.1016/j.ijthermalsci.2022.107505

27. Sheikholeslami, M., Said, Z., and Jafaryar, M. "Hydrothermal analysis for a parabolic solar unit with wavy absorber pipe and nanofluid", *Renew. Energy*, **188**, pp. 922–932 (2022).

28. Sheikholeslami, M., Jafaryar, M., Gerdroodbary, M.B., et al. "Influence of novel turbulator on efficiency of solar collector system", *Environ. Technol. Innov.*, **26**, (2022). https://doi.org/10.1016/j.eti.2022.102383

29. Sheikholeslami, M. and Farshad, S.A. "Nanoparticles transportation with turbulent regime through a solar collector with helical tapes", *Adv. Powder Technol.*, **33**(3), (2022). https://doi.org/10.1016/j.apt.2022.103510

30. Ahmad, S., Younis, J., Ali, K., et al. "Impact of swimming gyrotactic microorganisms and viscous dissipation on nanoparticles flow through a permeable medium- a numerical assessment", *J. Nanomater.*, **2022** (2022). https://doi.org/10.1155/2022/4888128

31. Ahmad, S., Akhter, S., Shahid, M.I., et al. "Novel thermal aspects of hybrid nanofluid flow comprising of manganese zinc ferrite $MnZnFe_2O_4$, nickel zinc ferrite $NiZnFe_2O_4$ and motile microorganisms", *Ain Shams Eng. J.*, **13**(5) (2022). https://doi.org/10.1016/j.asej.2021.101668

32. Akhter, S., Ahmad, S., and Ashraf, M. "Cumulative impact of viscous dissipation and heat generation on MHD Darcy-Forchheimer flow between two stretchable disks: Quasi linearization technique", *J. Sci. Arts*, **22**(1), pp. 219–232 (2022).

33. Shahid, M.I., Ahmad, S., and Ashraf, M. "Simulation analysis of mass and heat transfer attributes in nanoparticles flow subject to Darcy-Forchheimer medium", *Sci. Iran.*, **29**(4), pp. 1828–1837 (2022). DOI: 10.24200/SCI.2022.58552.5786

34. Ahmad, S., Ali, K., Haider, T., et al. "Thermal characteristics of kerosene oil-based hybrid nanofluids (Ag-$MnZnFe_2O_4$): A comprehensive study", *Front. Energy Res.*, **10** (2022). DOI: 10.3389/fenrg.2022.978819

35. Ali, K., Ahmad, S., Baluch, O., et al. "Numerical study of magnetic field interaction with fully developed flow in a vertical duct", *Alex. Eng. J.*, **61**(12), pp. 11351–11363 (2022).

36. Rasool, G., Shafiq, A., Khalique, C.M., et al. "MHD Darcy-Forchheimer nanofluid flow over a nonlinear stretching sheet", *Phys. Scr.*, **94**(10) (2014). https://doi.org/10.1088/1402-4896/ab18c8

Biographies

Maria Batool is a PhD Scholar under the supervision of Professor Ashraf and Dr. Ali at the Centre for Advanced Studies in Pure and Applied Mathematics, Bahauddin Zakariya University, Multan, Pakistan.

Shaheen Akhter recently completed her PhD in mathematics under the supervision of Professor Ashraf at the Centre for Advanced Studies in Pure and Applied Mathematics, Bahauddin Zakariya University, Multan, Pakistan. She is also a Lecturer at COMSATS University Islamabad, (Sahiwal Campus), Pakistan.

Sohail Ahmad has recently completed his PhD in Applied Mathematics from Centre for Advanced Studies in Pure and Applied Mathematics, Bahauddin Zakariya University, Multan 60800, Pakistan. He is working as a visiting faculty member at the Department of Mathematics, Muhammad Nawaz Sharif University of Engineering and Technology, Multan, Pakistan. His doctoral research investigates the heat and mass transfer, computational fluid dynamics, thermal analysis, advances in nanofluids, numerical study of flows through porous media, and magnetohydrodynamics. He takes a multidisciplinary approach that encompasses the fields of applied mathematics, biomechanics, fluid mechanics, mathematical physics, and mechanics. He is a potential reviewer of several international journals. Recently, he has authored more than twenty publications.

Kashif Ali received the PhD degree from Bahauddin Zakariya University, Multan 60800, Pakistan. He is working as an Assistant Professor at the Department of Mathematics, Muhammad Nawaz Sharif University of Engineering and Technology, Multan, Pakistan. He has numerous publications (more than 50) on his account in conferences and international journals of high impact factors. He is actively involved in studies on the numerical simulation of the fluid flow problems. Recently, he has developed various numerical methods such as Successive Over Relaxation (SOR) method, Finite Element Method (FEM), Quasi-linearization method, and Successive Under Relaxation (SUR) method in his publications. His research interests include multiphase fluid-particle dynamics, energy systems modeling, and nanofluids flow modeling.

Muhammad Ashraf is working as a Professor at the Centre for Advanced Studies in Pure and Applied Mathematics, Bahauddin Zakariya University, Multan, Pakistan. He has numerous publications (more than 70) on his account in international journals with high impact factors. He is actively involved in projects pertaining to the numerical simulation of the fluid flow problems. He has supervised and co-supervised many students of MPhil and PhD during his career. His research interests include fluid-particle dynamics, nanofluids flow modeling, transport in porous media, heat and mass transfer, magnetohydrodynamics, numerical analysis, fluid-particle separation, heat and fluids, computational fluid dynamics, modeling of fluid flow problems, nonlinear science, nanofluid, ferrohydrodynamic, electrohydrodynamic, and numerical simulation of mathematical models.